Performance and automation of ancient DNA capture with RNA hyRAD probes

Tomasz Suchan[1]*, Mariya A. Kusliy[1,2], Naveed Khan[1,3], Loreleï Chauvey[1], Laure Tonasso-Calvière[1], Stéphanie Schiavinato[1], John Southon[4], Marcel Keller[5], Keiko Kitagawa[6,7], Johannes Krause[8,9], Alexander N. Bessudnov[10], Alexander A. Bessudnov[11], Alexander S. Graphodatsky[2], Silvia Valenzuela Lamas[12], Jarosław Wilczyński[13], Sylwia Pospuła[13], Krzysztof Tunia[14], Marek Nowak[15], Magdalena Moskal-delHoyo[16], Alexey A. Tishkin[17], Alexander J.E. Pryor[18], Alan K. Outram[18], Ludovic Orlando[1]**

[1]Centre d'Anthropobiologie et de Génomique de Toulouse (CAGT), Université Paul Sabatier, Faculté de Médecine Purpan, Bâtiment A, 37 allées Jules Guesde, 31000 Toulouse, France

[2]Department of the Diversity and Evolution of Genomes, Institute of Molecular and Cellular Biology SB RAS, 630090, Academician Lavrentiev Avenue 8/2, Novosibirsk, Russia

[3]Department of Biotechnology, Abdul Wali Khan University, Mardan, 23200, Pakistan

[4]Earth System Science Department, B321 Croul Hall, University of California, Irvine, Irvine, CA 92697, USA

[5]Estonian Biocentre, Institute of Genomics, University of Tartu, Riia 23b, 51010 Tartu, Estonia

[6]SFB 1070 ResourceCultures, University of Tübingen, Tübingen, Germany.

[7]Department of Early Prehistory and Quaternary Ecology, University of Tübingen, Tübingen, Germany

[8]Department of Archaeogenetics, Max Planck Institute for the Science of Human History, 07745 Jena, Germany

[9]Max Planck Institute for Evolutionary Anthropology, 04103 Leipzig, Germany

[10]Lipetsk State Pedagogical P. Semyonov-Tyan-Shansky University. Lenin St., 42, Lipetsk, 398020, Russia

[11]Institute for the History of Material Culture, Russian Academy of Sciences, Dvortsovaia Naberezhnaia 18, Saint Petersburg, 191186, Russia

[12]Institución Milà i Fontanals de Humanidades, Consejo Superior de Investigaciones Científicas (IMF-CSIC), C/ Egipcíaquest 15, 08001, Barcelona, Spain

[13]Institute of Systematics and Evolution of Animals, Polish Academy of Sciences, Sławkowska 17 31-016 Kraków, Poland

[14]Institute of Archaeology and Ethnology, Polish Academy of Sciences, Sławkowska 17, 31-016 Kraków, Poland

[15]Institute of Archaeology, Jagiellonian University, Gołębia 11, 31-007 Kraków, Poland

[16]W. Szafer Institute of Botany, Polish Academy of Sciences, Lubicz 46, 31-512 Kraków, Poland

[17]Department of Archaeology, Ethnography and Museology, Altai State University, 656049, Lenin Avenue, 61, Barnaul, Russia

[18]Department of Archaeology, University of Exeter, Laver Building, North Park Road, Exeter, EX4 4QE, UK

* t.suchan@botany.pl

41 ** ludovic.orlando@univ-tlse3.fr

Abstract

DNA hybridization-capture techniques allow researchers to focus their sequencing efforts on pre-selected genomic regions. This feature is especially useful when analyzing ancient DNA (aDNA) extracts, which are often dominated by exogenous environmental sources. Here, we assessed, for the first time, the performance of hyRAD as an inexpensive and design-free alternative to commercial capture protocols to obtain authentic aDNA data from osseous remains. HyRAD relies on double enzymatic restriction of fresh DNA extracts to produce RNA probes that cover only a fraction of the genome and can serve as baits for capturing homologous fragments from aDNA libraries. We found that this approach could retrieve sequence data from horse remains coming from a range of preservation environments, including beyond radiocarbon range, yielding up to 146.5-fold on-target enrichment for aDNA extracts showing extremely low endogenous content (<1%). Performance was, however, more limited for those samples already characterized by good DNA preservation (>20-30%), while the fraction of endogenous reads mapping on- and off-target was relatively insensitive to the original endogenous DNA content. Procedures based on two, instead of a single round of capture, increased on-target coverage up to 3.6-fold. Additionally, we used methylation sensitive restriction enzymes to produce probes targeting hypomethylated regions, which improved data quality by reducing post-mortem DNA damage and mapping to multicopy regions. Finally, we developed a fully automated hyRAD protocol leveraging inexpensive robotic platforms to facilitate capture processing. Overall, our work establishes hyRAD as a cost-effective strategy to recover a set of shared orthologous variants across multiple ancient samples.

1. Introduction

In the last 15 years, High-Throughput DNA Sequencing (HTS) has found many applications in the genetic characterization of present-day biodiversity. HTS has also been extensively used to characterize past plant and animal communities, leveraging ancient DNA (aDNA) preserved both in sediments and sub-fossilized tissues (Leonardi et al., 2016; Orlando & Cooper, 2014). For example, aDNA metabarcoding has helped identify ecological shifts in relation to climatic change (Pedersen et al., 2016; Willerslev et al., 2014) and human activities, including pastoralism (Giguet-Covex et al., 2014), despite limitations due to the extensively degraded nature of aDNA (Dabney et al., 2013). While massive parallel sequencing of short DNA fragments (Goodwin et al., 2016) unveiled the full genome sequence of extinct organisms (even beyond the one million time range, van der Valk et al., 2021), aDNA libraries are frequently dominated by environmental microbial sources (Prüfer et al., 2010). Therefore, shotgun sequencing often provides a cost-ineffective strategy for characterizing past sequence variation at the genome scale.

In contrast to shotgun-sequencing, genome reduction approaches (*sensu* McCormack et al., 2013), including hybridization-based target-enrichment techniques (Kozarewa et al., 2015; Mamanova et al., 2010), are designed to focus sequencing efforts on a fraction of the genome only. These approaches not only reduce analytical costs but also maximize the chances to identify DNA present even in limited abundance (Slon et al., 2017). Therefore, target-enrichment provides an increasingly popular strategy for characterizing past biodiversity both at the community (Slon et al., 2017) and population (Mathieson et al., 2015) levels. The approach is also increasingly used for genetic monitoring of endangered populations for which only non-invasive material can be collected from very limited and/or heavily contaminated sources (Aylward et al., 2018; Fontsere et al., 2020).

One common limitation of hybridization-based genome reduction techniques pertains to probe design and synthesis. Typically, nucleic acid probes are designed on the basis of existing molecular panels, which are, however, not available across all taxa, especially amongst non-model organisms. Probe synthesis also entails significant costs that are generally commensurate to the number of loci targeted. A number of in-house procedures have been developed to limit probe production costs, through PCR amplification of number of target loci (Maricic et al., 2010; Peñalba et al., 2014), or *in vitro* transcription when aiming at the whole genome (Carpenter et al., 2013). HyRAD technologies have been recently proposed to fill the gap between those two alternatives, allowing users to scale up probe production to their research question and sequencing capacity (Schmid et al., 2017; Suchan et al., 2016). The methodology leverages the versatility of RAD sequencing, which targets genomic regions flanking (Peterson et al., 2012) or encompassing (Baird et al., 2008) user-selected restriction sites. In hyRAD, enzymatic restriction is first applied to fresh DNA from a set of individuals of the focal or closely-related species. Digested DNA fragments are then immortalized to produce target enrichment probes on-demand for in solution aDNA capture (Suchan et al., 2016).

Despite reported success on plant and animal museum specimens (Boucher et al., 2016; Crates et al., 2019; Gauthier et al., 2020; Lang et al., 2020; Linck et al., 2017; Schmid et al., 2018), the full potential of hyRAD to characterize past molecular diversity remains largely unexplored. Currently, only one study retrieved aDNA over the thousand-year time scale from ~7,000 year-old pine needles that were preserved in the lake sediments (Schmid et al., 2017). The suitability of hyRAD to (1) other preservation conditions, (2) deeper time ranges, and (3) calcified material, such as bones, teeth and shells, which represent the dominant fraction of the fossil record is, thus, unknown.

In this study, we applied hyRAD for the first time to ancient osseous material going beyond the radiocarbon time range and spanning various environmental conditions (from Tunisia, Poland and Russia; Tab. 1). We benchmarked hyRAD protocols including one or two-rounds of capture and different combinations of restriction enzymes. These included methylation-sensitive enzymes with the aim to target hypomethylated genomic regions and limit the impact of post-mortem DNA damage (Seguin-Orlando et al., 2015; Smith et al., 2015), while diverting sequencing efforts from the most repetitive, hypermethylated, fraction of the genome (Karam et al., 2015; Larsson et al., 2013). We also developed and validated an automated protocol for targeted capture on Opentrons OT-2 liquid-handling robots to minimize hands-on time and the risk of experimental errors. Overall, the procedures presented in this study successfully retrieved authentic aDNA data from material beyond the radiocarbon time range and could achieve up to 146.46-fold enrichment of on-target reads on DNA extracts originally showing 0.34% endogenous DNA. The approach was successful in retrieving orthologous DNA fragments from different samples, with limited sequencing efforts.

2. Methods

2.1. DNA extraction and sample library preparation

The samples consisted of 12 bone or tooth material, ranging from Late Pleistocene to the 4th century CE (Common Era), from Tunisia, Poland and Russia. They were selected following shallow shotgun sequencing to encompass almost an entire range of endogenous DNA content (0.34-73.78%; Tab. 1). DNA extraction followed Gamba et al. (2016) with modifications from Fages et al. (2019). Extracted DNA was treated with USER mix (Uracil-Specific Excision Reagent, New England Biolabs - NEB) prior to DNA library construction, following Fages et al. (2019). A total of 14.9 µl of USER-treated aDNA extract was used for

library preparation according to the modified Meyer & Kircher (2010) protocol presented in Fages et al. (2019)**,** including one 6-bp external index (Orlando et al., 2013) and two 7-bp internal indices from Rohland et al. (2015) (Fig. S1A). In order to ensure sufficient amounts of DNA templates for hyRAD capture, each of the 12 DNA libraries were amplified in two successive rounds of PCR. First, 3 µl of library was used within a 25 µl reaction with of 0.2 µM of IS4 primer, 0.2 µM of indexing primer (Meyer & Kircher, 2010), 0.5 µg/µl of BSA (NEB), 1 U of AccuPrime Pfx polymerase (ThermoFisher Scientific) and 1x AccuPrime buffer. PCR consisted of 5 min denaturation at 95°C, followed by 11 cycles of 15 s at 95°C, 30 s at 60°C, 30 s at 68°C, and a final elongation for 5 min at 68°C. The number of PCR cycles for the second reaction was determined using qPCR and the samples were re-amplified either in two (samples KB2017, PLMie3, LOG3, DIV9, SV2019-22, SV2019-18, PLKaz4, PLKaz1; used for the capture with *PstI-MseI* probes only) or 16 parallel PCRs (samples PLMie10, PLSla2, PLMie8, PLKaz2; used for the capture with all three types of the probes and the automated capture test, see below), in order to obtain the required amount for the capture. The second amplification round was carried out using the IS5_reamp.P5 and IS6_reamp.P7 primers (Tab. S1) from Meyer & Kircher (2010) and the same PCR conditions as above, except that the primer concentration was 0.4 µM and only 1 µl of DNA template was used. For each sample, PCR replicates were pooled, purified and concentrated into 10 µl (for duplicate reactions) or 80 µl (for multiplicate reactions), using MinElute columns (Qiagen).

2.2. Probe library preparation and probe production

Probe production was based on previous hyRAD protocols (Schmid et al., 2017), which rely on *in vitro* transcription of the probe library molecules containing T7 RNA polymerase promoter. Overall, high-molecular weight DNA extracts (2 µg) from a modern domesticated

160 horse were subject to double enzymatic restriction before being ligated to two adapters, each
161 showing terminal ends complementary to one restriction site (Fig. S1B). Different
162 combinations of restriction enzymes were selected to provide different levels of genome
163 reduction. The *PstI-MseI* combination targeted 6-bp- and 4-bp-long restriction sites,
164 respectively, and therefore was expected to produce fewer digested fragments than *MspI-MseI*
165 and *HpaII-MseI* combinations, which both build on 4-bp-long restriction sites only. The latter
166 two combinations were also selected to target genomic regions showing different DNA
167 methylation background. Both *HpaII* and *MspI* enzymes target the same DNA restriction site
168 (C|CGG) but *HpaII* does not cleave DNA when the central CpG dinucleotide is methylated, in
169 contrast to *MspI*.

170 Each digestion reaction used 40 U of *PstI*-HF (or *MspI*/*HpaII*, NEB) and 20 U of *MseI* (NEB)
171 in the CutSmart buffer for 3 h at 37°C in 100 µl. The reaction was purified using AMPure
172 beads (Beckman Coulter), with a bead-to-liquid ratio of 2:1 and eluted in 20 µl of Tris 10
173 mM. The purified DNA was then used in a 3 h ligation reaction at 16°C with 800 U of T4
174 DNA ligase (NEB) and 0.7 µM of each adapter (P1 and P2, see Tab. S1), with a final volume
175 of 28 µl. Following ligation and purification with AMPure beads (bead-to-liquid ratio =
176 1.5:1), DNA templates were selected within the 190-390 bp size range using the Blue Pippin
177 instrument and 2% agarose cassettes with external marker (Sage Science), which corresponds
178 to inserts of ~100-300 bp. A further purification step allowed the elimination of those probe
179 library constructs that did not incorporate the P2 adapter. This was achieved using the biotin
180 group present in the P2 capture adapter and streptavidin-coated beads (MyOne C1
181 Dynabeads, Invitrogen). A total of 40 µl of the beads was first washed and resuspended in 2x
182 TEN buffer (10mM Tris-HCl, 1mM EDTA, 2M NaCl), then combined with 40 µl of DNA,
183 incubated rotating for 15 min, separated on magnet, washed three times with 1x TEN buffer

and resuspended in 15 µl of water. Finally, the probe library constructs showing both P1 and P2 adapters were PCR amplified in a single reaction using KAPA HiFi HotStart ReadyMix (Roche), 0.6 µM of IS4 primer and indexing primer (Meyer & Kircher, 2010), and 7.5 µl of the bead solution obtained in the previous step. The PCR conditions were the same as for aDNA libraries, except that 14 cycles were used. The probe library was purified using AMPure beads (bead-to-liquid ratio = 1:1) and eluted in 20 µl of 10 mM Tris. Half of the probe library was kept for sequencing while the rest was digested with 1.5 U of *MseI* in 15 µl reaction for 3 h at 37°C to remove the P2 adapter prior to the probe production through *in vitro* transcription. Adapter removal was confirmed and concentration estimated by running the sample on TapeStation 4200 instrument (Agilent). RNA probes were then synthesized following *in vitro* transcription using the HiScribe T7 High Yield RNA Synthesis Kit (NEB) according to the manufacturer's instructions, with 1/3 of UTP molarity as biotin-16-UTP (Roche), and 2 µl of the DNA template in 40 µl reaction, for 16 h at 37°C. Each reaction was then subject to TurboDNAse (Thermo Fisher) treatment at 37°C for 30 min to remove remaining DNA templates and purified on RNEasy Mini column (Qiagen) using standard procedure, except that 675 µl of ethanol was used with RNA and RTL buffer mix prior to column loading step to ensure that RNA probes of all possible lengths were retained. The purified probes were eluted in 50 µl of EB buffer (Qiagen) and supplemented with 2.5 µl of SUPERase-In (Thermo Fisher).

HyRAD capture requires the use of blocking RNA oligonucleotides that are complementary to the Illumina P5 and P7 adapters present in aDNA libraries (Fig. S1A). Blocking RNA were synthesized by annealing synthetic BO.P5 and BO.P7 DNA oligonucleotides with anoither oligonucleotide consisting of the P7 promoter sequence (Tab. S1; Carpenter et al., 2013) at 50 µM concentration and using 1 µl of annealed template for *in vitro* transcription with the

HiScribe T7 High Yield RNA Synthesis Kit (NEB). Separate transcription reactions were carried out for each blocking RNA and subject to TurboDNAse treatment and RNEasy Mini column purification, as above.

2.3. Hybridization capture

Hybridization conditions closely followed MyBaits v3 protocol (MYcroarray, USA; http://www.mycroarray.com/mybaits/manuals.html) and the work from Suchan et al. (2016) and Cruz-Davalos et al. (2017). For each reaction, 500 ng of DNA library was mixed with a blocking mix consisting of blocking RNA (0.55 µM), RNA probes (500 ng), human Cot-1 DNA (2.3 µg) and salmon sperm DNA (2.3 µg), and denatured for 5 min at 95°C. The temperature was then lowered to 55°C for hybridization (Cruz-Dávalos et al., 2017) and the pre-warmed hybridization solution with RNA probes added. The final hybridization reaction included 5.4x SSPE (equivalent to 0.8 M NaCl), 0.15% SDS, 5.25x Denhardt's solution, 0.9 U of SUPERase-In (Thermo Fisher) and 13 mM EDTA (including the one present in the SSPE buffer). The 55°C incubation for the first round of capture was carried out for 40 h but only for 16 h during the second round, as the first round already considerably reduced the proportion of non-focal library material (Fig. 1).

Next, captured DNA fragments were immobilized during 30 min at 55°C by adding 30 µl of streptavidin-coated beads (Dynabeads C1, Thermo Fisher) resuspended in 70 µl of TEN buffer (10 mM Tris-HCl pH 7.5, 1 mM EDTA, 1M NaCl). Beads were separated on the magnet, resuspended and incubated for 15 minutes in 180 µl of 1x SSC/0.1% SDS, resuspended and incubated three times for 10 minutes with 180 µl of 0.1x SSC/0.1% SDS, and finally, resuspended in 30 µl of water.

All samples were subject to capture with *PstI-MseI* probes. Four samples (PLMie10, PLSla2, PLMie8, PLKaz2) were also captured on two additional sets of probes (*MspI-MseI* and *HpaII-MseI*). Since probe libraries contain Illumina sequencing adapters, they could be sequenced prior to *in vitro* transcription in order to identify the genomic locations (targets) subject to enrichment (Fig. S1B). The aDNA libraries were sequenced prior to and following one (samples PLMie10, PLSla2, PLMie8, and PLKaz2) or two rounds of enrichment (all the samples). The four samples sequenced after the first and second round of capture were used to assess the impact of successive rounds of capture. Specifically, the sample libraries obtained following one round of capture were subject to either a second round of capture after re-amplification for approximately 500 ng of DNA, or to sequencing following fewer PCR amplification cycles. The number of PCR cycles was determined by qPCR and ranged from 12 to 20 for preparing the second round of capture, 5-15 for sequencing after the first round of capture and 3-4 for sequencing after the second. PCRs were performed using KAPA HiFi HotStart ReadyMix, 7.5 µl of the beads solution after the capture and wash steps, and 0.5 µM of IS5_reamp.P5 and IS6_reamp.P7 primers (Tab. S1) from Meyer & Kircher (2010). All resulting sample and probe libraries were sequenced on the Illumina MiniSeq instrument, using 2 × 80 bp High-Output Kit.

The detailed protocol is available as a supplementary material.

2.4. Protocol automation

The automation protocol was implemented using Opentrons OT-2 robot (opentrons.com; also see May, 2019), equipped with magnetic and PCR modules, and includes all steps underlying hybridization capture, namely: (1) hybridization of aDNA libraries with the blocking mix, pre-warming and addition of probes; (2) incubation in the Opentrons PCR module, and; (3) pre-warming of all washing buffers and performing washing by moving the samples to the

Opentrons magnetic module for bead separation and buffer change, and back for incubation on the PCR module. The efficacy of the automated capture was assessed by comparison to the performance achieved manually following two-round captures on four samples (PLMie10, PLSla2, PLMie8, and PLKaz2).

2.5. Data analysis

Paired-end sequence data obtained from probe libraries were filtered and trimmed using cutadapt v2.10 (Martin, 2011). We only kept those read pairs showing a fragment of the P1 adapter (consisting of the T7 promoter and the restriction cut-site) at the beginning of the first read, and the second cut-site at the beginning of the second read. For the P1 adapter, no more than 3 errors were allowed, including at best one base indel at read start. For the second adapter, full sequence match to the second cut-site and full overlap thereof were enforced. The resulting trimmed read pairs were then aligned against the horse EquCab3 reference genome (Kalbfleisch et al., 2018) using paleomix v1.3.2 (Schubert et al., 2014) and both BWA v0.7.17 backtrack algorithm (Li et al., 2009) and Bowtie2 v2.3.4.1 (Langmead & Salzberg, 2012). For Bowtie2, we used the mapping parameters recommended by Poullet & Orlando (2020), while default parameters were used with BWA. All read alignments were then filtered to a minimal mapping quality of 25. While read alignment was carried out using both BWA and Bowtie2 with similar outcomes, we chose the latter for subsequent analyses, based on generally higher numbers of mapped collapsed reads, in line with previous work (Cahill et al., 2018; Poullet & Orlando, 2020) (Tab. S2; Fig. S2).

For DNA sequences obtained from aDNA libraries, similar procedures were used, except that (1) AdapterRemoval v 2.3.1 (Schubert et al., 2016) was used for read trimming and collapsing instead of cutadapt; (2) seeding was disabled during BWA mapping (Schubert et al. 2012); (3) rmdup_collapsed from Paleomix was used for removing PCR duplicates for collapsed and

Picard tools v2.18.0 (http://broadinstitute.github.io/picard/) for uncollapsed reads, and; (4) post-mortem DNA damage was assessed using mapDamage v2.2.1 (Jónsson et al., 2013) and PMDtools v0.50 (Skoglund et al., 2014).

The expected number and size of DNA fragments obtained following enzymatic digestion were estimated *in silico* applying fragmatic (Chafin et al., 2018) to the EquCab3.0 reference genome. Here, all three combinations of enzymatic restrictions could be investigated using two analyses only, as *HpaII* and *MspI* target the same restriction site. Preseq v.2.0.3 (Daley & Smith, 2013) functions c_curve (step size in extrapolations = 10,000) and lc_extrap (maximum extrapolation = 50,000,000, step size in extrapolations = 10,000) were used to estimate library complexity profiles.

Comparison between the different experimental conditions was carried out by random sampling identical numbers of reads for each given sample for all the treatments (to the lowest number of reads obtained for each sample (range = 88,013-690,062, mean = 464,500).

The following statistics were calculated for the libraries pre- and post-capture, using custom scripts based on the samtools v.1.10 (Li et al., 2009) and bedtools v2.29.2 (Quinlan & Hall, 2010): the fraction of endogenous DNA (number of reads mapping to the reference genome / number of raw reads); the fraction of unique endogenous DNA; the amount of PCR duplicates; the fraction of on-target reads (reads showing at least 1-bp overlap with probe coordinates); the fraction of unique on-target reads; the average depth-of-coverage for unique on-target reads; the size distribution of the uniquely-mapped fragments (based on collapsed read pairs only, as these ensure that full aDNA fragments were sequenced); the GC content of the uniquely-mapped reads and; the number of on-target sites with depth > 0 (following PCR duplicate removal). We have also plotted the size distribution of on-target reads (based only on collapsed reads for precision), and analyzed enrichment folds (number of reads mapped

after the procedure/number of reads mapped prior to the procedure) for captures with *PstI-MseI* probes. For probe reads, additional statistics such as the %GC content, CpG content and fragment length were calculated. When probe reads were not overlapping, GC and CpG content were calculated based on the underlying genomic region on the reference genome.

To assess the authenticity of the obtained sequences we used mapDamage (Jónsson et al., 2013) and PMD tools (Skoglund et al., 2014) to quantify nucleotide misincorporations. For datasets obtained using *MspI-MseI* and *HpaII-MseI* probes, we also used PMD tools to quantify CpG→TpG mis-incorporation rates. Such transitions generally derive from post-mortem cytosine deamination (Briggs et al., 2007). However, methylated CpG dinucleotides that are deaminated post-mortem are protected from USER-treatment and sequenced as TpG dinucleotides (Hanghøj et al., 2016), in contrast to unmethylated CpG dinucleotides that are converted into UpG dinucleotides and eliminated following USER-treatment (Hanghøj et al., 2016). Therefore, CpG→TpG mis-incorporation rates calculated on sequencing data generated following USER-treatment offer an opportunity to track the overall methylated level of the genomic regions effectively enriched. We also assessed the fraction of mappable reads obtained using each probe set, and the proportion of reads flagged as multimapping to determine whether the targeted regions could represent genomic regions with non-average numbers of repeated elements.

For all 12 samples captured on *PstI-MseI* probes, genomic variants were called with freebayes v1.2.0 (Garrison & Marth, 2012) using sequence data obtained pre-capture and after second the round of capture, with the following options: --hwe-priors-off --no-population-priors --genotype-qualities --min-base-quality 3 --min-mapping-quality 25, and filtered on the genotype level with vcffilter for depth > 3 and genotype quality > 20 using vcffilter (vcflib 1.0.1; https://github.com/vcflib/vcflib). Data missingness was calculated with VCFtools v.0.1.16 (Danecek et al., 2011).

3. Results

3.1. Study design and probe libraries

Over the last few years, our laboratory has undertaken an extensive genomic characterization of ancient horse specimens, which has resulted in an assessment of aDNA preservation levels in over 2,000 osseous remains, spread across the last 100,000 years in North Africa and Eurasia (Fages et al., 2019; Orlando, 2020). This allowed us to select 12 aDNA extracts representing three biomolecular preservation contexts and showing an entire range of endogenous DNA (from 0.34% to 73.78%; Tab. 1). Target-enrichment was applied using three panels of hyRAD probes prepared from the genomic DNA extract of a single modern horse mare that was digested by different combinations of restriction enzymes (*PstI-MseI*, *MspI-MseI* and *HpaII-MseI*). The experimental procedures described here allowed for the preparation of extensive amounts of RNA probes. For instance, we obtained 92 µg, 51 µg and 13.74 µg of RNA from 2 µl of digested *PstI-MseI*, *MspI-MseI,* and *HpaII-MseI* probes library, respectively. Digesting and using the full volume of probe libraries would, thus, theoretically allow users to perform approximately 400-2,700 capture reactions.

The size distribution of probe library templates was highly similar to that predicted after *in silico* digestion of the horse reference genome within the selected size range (Fig. S4). From limited sequencing efforts (502,815 read pairs), we could estimate that 1.81% (*PstI-MseI*), 2.07% (*MspI-MseI*) and 1.55% (*HpaII-MseI)* of the horse genome was represented in the probe libraries (Tab. 2). This equates to approximately 21-29% (1.55%/7.16% and 2.07%/7.16%) to 38% (1.81%/4.77%) of the maximal genome coverage expected according to *in silico* digestion. Preseq calculations (Fig. S5, S6; Daley & Smith, 2013) indicated that moderate sequencing efforts (~5-10 million read pairs) would be sufficient to reveal the full probe library content.

HyRAD probes were found evenly distributed across all autosomes and the X chromosome (Fig. S7, S8), while no alignments were retrieved against Y-chromosomal contigs, in line with probes originating from a mare. Additionally, mitochondrial DNA sequences were extremely rare within the probe libraries (9 for *HpaII* a, 6 for *MspI* and absent for *PstI*; Tab. S3) as expected from the (nearly) absence of *in silico*-predicted digested fragments (absent for *PstI-MseI* and 10 for *MspI/HpaII-MseI*).

3.2. Enrichment efficacy

Sequence alignments showed the hallmark of post-mortem DNA degradation following USER-treatment, including mild C→T mis-incorporation rates towards read termini (Fig. S10) and fragmentation at cytosine residues (ie. those are deaminated into uracil after death and cleaved by USER-treatment; Rohland et al. 2015). This indicated that the experimental procedure followed in this study succeeded in retrieving authentic aDNA sequence data.

We first assessed hyRAD performance on four specimens by comparing the sequence data obtained following shotgun sequencing and after one or two successive rounds of capture (Fig. 1). HyRAD capture resulted in increased overall levels of endogenous DNA present in the three aDNA libraries characterized by low starting endogenous DNA (0.34% to 6.55% pre-capture). This was true for all three probe types, even though these only covered 4.77% to 7.16% of the horse genome. For these three samples, the number of horse DNA fragments increased dramatically following one round of enrichment (2.73-21.63-fold for unique reads, and; 2.27-22.62-fold considering PCR duplicates; Chi-squared test testing four samples before vs. the same samples after capture, p-values $< 2.2^{-16}$ for all the probe types). Endogenous DNA content increased even further following a second round of enrichment for the two samples (on *PstI-MseI* probes) or three samples (for the rest of the probes) with the lowest endogenous DNA content (4.00 to 53.13-fold, 4.17 to 73.07-fold, for unique reads and

375 considering PCR duplicates , respectively; Chi-squared test as above, *p*-values < 2.2^{-16} for all
376 the probe types). Endogenous DNA content was reduced after the second capture for the
377 PLMie8 sample on *PstI-MseI* probes (6.55% original endogenous DNA content), from 3.10 to
378 2.64-fold for unique reads and 3.12 to 2.75-fold considering PCR duplicates. However using
379 the robotic protocol, the values after the second capture were higher (4.74 and 4.95-fold,
380 respectively), pointing to the possible variability of the procedure outcome and benefits of
381 automation (see below). Sample PLKaz2, which was characterized by the highest endogenous
382 DNA content pre-capture (73.59%), stands as an exception as endogenous DNA content was
383 reduced after one round (0.65-0.74%) or two capture rounds (0.56-0.67%). This reduction
384 was not present reads were not filtered for mapping quality (Fig. S10) and accompanied by a
385 dramatic decrease in mean mapping quality of the aligned reads (Fig. S11, Wilcoxon rank-
386 sum test, *p*-values = 2.2^{-16} for all the probe types), suggesting that capture increased the
387 sequencing of genomic regions found in multiple copies across the genome.

388 HyRAD-enriched horse DNA sequences did not map randomly across the genome but were
389 instead preferentially located on probe regions (Fig. 1), resulting in on-target enrichment
390 factors for unique reads of 1.03 to 52.88-fold (median = 6.56-fold). Performing two rounds of
391 hyRAD capture increased on-target coverage further (1.15 to 146.46-fold; median = 16.90-
392 fold; Chi-squared test, *p*-values < 2.2^{-16} for all the probe types), despite proportions of PCR
393 duplicates especially increased in the three specimens showing limited endogenous DNA
394 levels prior to capture. Overall, performing two capture rounds resulted in 1.52 to 173.80-fold
395 increase in genomic sites covered at least once uniquely (Fig. 2), which demonstrates the
396 capacity of hyRAD capture to significantly reduce sequencing costs pertaining to the
397 characterization of a pre-selected fraction of the genome in ancient samples. The expected
398 reduction in costs is two-fold. First, sequencing costs are directly proportional to the
399 enrichment-fold, which is rapidly cost-effective relative to the cost incurred per capture

400 reaction (15EUR). Second, the protocol presented here for in-house probe production costs
401 around 120 EUR for 400-2,700 capture reactions, which outperform commercial production
402 for target spaces representing substantial genome fractions.

403 Both the size and the %GC content of the endogenous DNA molecules sequenced increased
404 with the number of hyRAD capture rounds (Fig. 3). This is on par with the previously
405 reported performance of target-enrichment using in-solution synthetic RNA (Cruz-Dávalos et
406 al., 2017), with longer and %GC-richer templates favoring probe-to-target annealing.

407 We next enriched 8 additional samples on *PstI-MseI* probes to investigate hyRAD
408 performance across an almost continuous range of endogenous DNA preservation levels
409 following two capture rounds (Fig. 4). This experiment illustrated the trade-off between on-
410 target enrichment rates and the original endogenous DNA library content (Fig. 4; Tab. S5). It
411 showed that hyRAD capture performs the best when initial endogenous DNA content (<30%)
412 and initial PCR duplicate levels are low (>5.63% in our case). The proportion of on-
413 target/endogenous reads was, however, relatively insensitive to initial endogenous DNA
414 content pre-capture. Importantly, enrichment folds increased with the fraction of large
415 (>50bp) endogenous fragments available pre-capture (Fig. 5). This indicates that the
416 prominent limiting factor for aDNA hyRAD capture is the extent of DNA fragmentation
417 ongoing after death, hence, the availability of DNA templates of sufficient size during
418 enrichment.

419 The increased on-target coverage achieved using hyRAD translated into a higher proportion
420 of shared genomic loci amongst samples (Fig. 6A). With our limited sequencing efforts,
421 approximately 100,000 sites were common to four samples following shotgun sequencing and
422 no sites were shared across all samples. With equivalent sequencing efforts, approximately
423 100,000 sites were common to 11 samples and 2,846 were shared across all samples. This led

to the identification of 87 variants, 44 of which were present in at least two samples. In contrast, prior to capture, we only detected three variants that were private to two individual samples (Fig. 6B,C). The total number of variants identified per sample also increased up to 52 following two rounds of hyRAD capture (Fig. 6C). This demonstrates the capacity of hyRAD capture to provide shared orthologous sequence information across multiple samples. PreSeq calculations (Daley & Smith, 2013) predicted that the full content of aDNA libraries content could be revealed following sequencing of ~1.5-2 million read pairs for the libraries captured on *PstI-MseI* probes, except the libraries of high PCR duplication rate for which 0.5 million read pairs would be sufficient (Fig. S12).

3.3. Scaling and DNA methylation sensitivity

The choice of restriction enzymes allows hyRAD users to scale their experimental design according to the question of interest and sequencing capacity. By choosing restriction enzymes that are sensitive to DNA methylation (eg. *HpaII*), they can also target less repetitive hypomethylated regions (Karam et al., 2015; Larsson et al., 2013). This may be especially interesting for aDNA characterization as such regions are less prone to post-mortem DNA damage (Smith et al. 2014, Seguin-Orlando et al. 2015). To demonstrate this, we compared on-target CpG→TpG mis-incorporation rates as a measure of post-mortem cytosine deamination, following one and two rounds of hyRAD capture with *HpaII-MseI* probes (methylation-sensitive) and *MspI-MseI* probes (methylation-insensitive). These rates were indeed lower when the methylation-sensitive combination was used (Fig. 7), but not when including off-target reads (Fig. S13), confirming that the genomic fraction effectively enriched was associated with lower post-mortem DNA damage. The number of on-target reads flagged as multimapping was also considerably smaller when the methylation-sensitive combination was used (Fig. S14; Tab. 2). This was not true for off-target reads, confirming

that capturing hypomethylated regions can indeed help focus on genomic regions with reduced repetitive content.

3.4. Protocol automation

Automated solutions to aDNA analyses gained increasing interest over the last few years (Rohland et al., 2015; Slon et al., 2017), with the benefit of increased efficiency and reproducibility (Holland & Davies, 2020). However, investment costs for acquiring liquid-handling robots can be extremely prohibitive and not available outside of large-scale facilities. To provide an automation solution for most laboratories, we developed an automated hyRAD protocol that can be run of the inexpensive liquid-handling devices produced by Opentrons. Our automated implementation reduced hands-on time to 30 minutes per capture session, *versus* 3 hours when carried out manually by skilled laboratory staff, while showed performance similar (Fig. 10). The developed protocol is available as at https://github.com/TomaszSuchan/opentrons-hyRAD.

4. Discussion

In this study, we investigated for the first time the potential of hyRAD target-enrichment for aDNA extracted from osseous remains. First, we modified the original hyRAD protocol in order to produce RNA probes from the ddRAD-seq templates, by including T7 polymerase promoter in the library adapter's sequence, as in Schmid et al. (2017). This modification has several benefits over the original approach (Suchan et al., 2016). First, using RNA probes reduces the risk of contamination of aDNA libraries by the probes during capture. Second, RNA-DNA heteroduplexes show higher affinity than DNA-DNA homoduplexes (Lesnik & Freier, 1995), thus, improving capture efficacy (Furtwängler et al., 2020). Finally, the T7 polymerase reaction allowed us to obtain sufficient amounts of RNA probes for carrying out thousands of capture reactions from relatively modest amounts of starting DNA. We, thus,

solved the main limitation of the original hyRAD protocol, which required many subsequent PCR amplifications to obtain sufficient amounts of capture probes (Suchan et al., 2016).

We assessed hyRAD performance using three types of probes and one single or two rounds of enrichment. We found that the second round of enrichment consistently improved on-target recovery, despite also dramatically increasing the proportion of PCR duplicates. This was especially the case for low endogenous DNA content samples, consistent with previous research (Fontsere et al., 2020; Hernandez-Rodriguez et al., 2018). We also confirmed previous reports of limited enrichment for aDNA libraries showing high starting endogenous DNA content (Cruz-Dávalos et al., 2017). We show that this was mainly driven by the dramatic drop of mean mapping qualities for the captured reads likely resulting from increased proportions of repeated elements post-capture.

On-target enrichment reached up to 146-fold for the sample with the lowest endogenous DNA content (0.34%) and around 3.5-fold for samples with 13.90 and 20.64% of endogenous DNA content (not counting samples with high initial PCR duplication rates), which reduces sequencing costs proportionally. Enrichment folds were, however, limited to around 1.4-1.8 for samples with >30% endogenous DNA (Fig. 4; Tab. S5), which is lower than what reported for commercial capture protocols (Cruz-Dávalos et al., 2017). Commercial protocols, however, are based on synthetic probes, and can be carefully designed to represent optimal probe molecular features that cannot be controlled with hyRAD. Our experimental conditions were also less stringent (55°C incubation for 40 and 16 h) in line with the recommendations of Cruz-Dávalos et al. (2017) on synthetic RNA probes. Further work is necessary to assess whether more stringent annealing conditions could overcome some of the limitations of our current procedure.

The size distribution of horse DNA fragments increased with each round of enrichment, as previously shown for aDNA and environmental DNA (Cruz-Dávalos et al., 2017; Enk et al., 2014). This suggests that more limited enrichment success can be expected for aDNA libraries characterized by extreme fragmentation. The enrichment potential of a given set of samples can be assessed prior to capture following shallow shotgun sequencing so as to gauge for the presence of endogenous DNA fragments of a relatively long size (*e.g.* 80 bp and above) and low duplication rates.

We also demonstrated that probe preparation with methylation-sensitive restriction enzymes could help focus sequencing efforts on hypomethylated regions, and limit both the fraction repetitive regions sequenced (Karam et al., 2015; Larsson et al., 2013) and the amounts of nucleotide mis-incorporations pertaining to post-mortem DNA damage (Smith et al. 2014, Seguin-Orlando et al. 2015). Therefore, the hyRAD procedure described can not only achieve a cost-effective characterization of orthologous genomic regions across a set of samples but can also improve the underlying sequence quality. It can also reduce hands-on time, and improve experimental reproducibility and traceability when automated. Our approach appears especially appropriate for ancient samples characterized with low endogenous DNA content but not excessively fragmented. It may provide future avenue for the genetic characterization of environmental (Wilcox et al., 2018) and non-invasive samples (*e.g.* feces, Fontsere et al., 2020), which are both characterized by limited DNA amounts of the species of interest.

Data Availability

The datasets generated for this study can be accessed in the ENA (Accession Number PRJEB43744). The laboratory protocol is available at [WILL BE AVAILABLE ONLINE UPON ACCEPTANCE, NOW ATTACHED AS SUPPLEMENTARY FILE].The program

for piloting the Opentrons OT-2 robot can be accessed at https://github.com/TomaszSuchan/opentrons-hyRAD.

Author contributions

Designed and conceived the study: TS, LO. Performed wet-lab work: TS, MK, NK, LC, LTC, SS. Provided samples, material and reagents: MK, KK, AB, AAB, ASG, SVL, JW, SP, KT, MN, MMdH, AAT, AJEP, AK, LO. Analyzed data: TS, LO. Interpreted the data: TS, LO. Wrote the article: TS, LO, with input from all co-authors.

Acknowledgments

We thank all CAGT members for discussion and help, in particular Stefanie Wagner for initial training in the ancient DNA facilities. This project has received funding from: the University Paul Sabatier IDEX Chaire d'Excellence (OURASI); the CNRS Programme de Recherche Conjoint (PRC); the CNRS International Research Project (IRP AMADEUS); the European Union's Horizon 2020 research and innovation programme under the Marie Skłodowska-Curie grant agreement No 797449; the Russian Foundation for Basic Research, project No. 19-59-15001 "*Horses and their importance in the life of the ancient population of Altai and adjacent territories: interdisciplinary research and reconstruction*" ; the European Research Council (ERC) under the European Union's Horizon 2020 research and innovation programme (grant agreement 681605).

References

Aylward, M. L., Sullivan, A. P., Perry, G. H., Johnson, S. E., & Louis, E. E. (2018). An environmental DNA sampling method for aye-ayes from their feeding traces. *Ecology and Evolution*, *8*(18), 9229–9240. https://doi.org/10.1002/ece3.4341

Baird, N. A., Etter, P. D., Atwood, T. S., Currey, M. C., Shiver, A. L., Lewis, Z. A., Selker, E. U., Cresko, W. A., & Johnson, E. A. (2008). Rapid SNP discovery and genetic mapping using sequenced RAD markers. *PloS One*, *3*(10), e3376. https://doi.org/10.1371/journal.pone.0003376

Boucher, F. C., Casazza, G., Szövényi, P., & Conti, E. (2016). Sequence capture using RAD

probes clarifies phylogenetic relationships and species boundaries in Primula sect. Auricula. *Molecular Phylogenetics and Evolution*, *104*, 60–72. https://doi.org/10.1016/j.ympev.2016.08.003

Briggs, A. W., Stenzel, U., Johnson, P. L. F., Green, R. E., Kelso, J., Prüfer, K., Meyer, M., Krause, J., Ronan, M. T., Lachmann, M., & Pääbo, S. (2007). Patterns of damage in genomic DNA sequences from a Neandertal. *Proceedings of the National Academy of Sciences of the United States of America*, *104*(37), 14616–14621. https://doi.org/10.1073/pnas.0704665104

Cahill, J. A., Heintzman, P. D., Harris, K., Teasdale, M. D., Kapp, J., Soares, A. E. R., Stirling, I., Bradley, D., Edwards, C. J., Graim, K., Kisleika, A. A., Malev, A. V., Monaghan, N., Green, R. E., & Shapiro, B. (2018). Genomic Evidence of Widespread Admixture from Polar Bears into Brown Bears during the Last Ice Age. *Molecular Biology and Evolution*, *35*(5), 1120–1129. https://doi.org/10.1093/molbev/msy018

Carpenter, M. L., Buenrostro, J. D., Valdiosera, C., Schroeder, H., Allentoft, M. E., Sikora, M., Rasmussen, M., Gravel, S., Guillén, S., Nekhrizov, G., Leshtakov, K., Dimitrova, D., Theodossiev, N., Pettener, D., Luiselli, D., Sandoval, K., Moreno-Estrada, A., Li, Y., Wang, J., … Bustamante, C. D. (2013). Pulling out the 1%: Whole-Genome Capture for the Targeted Enrichment of Ancient DNA Sequencing Libraries. *The American Journal of Human Genetics*, *93*(5), 852–864. https://doi.org/10.1016/j.ajhg.2013.10.002

Chafin, T. K., Martin, B. T., Mussmann, S. M., Douglas, M. R., & Douglas, M. E. (2018). FRAGMATIC: In silico locus prediction and its utility in optimizing ddRADseq projects. *Conservation Genetics Resources*, *10*(3), 325–328. https://doi.org/10.1007/s12686-017-0814-1

Crates, R., Olah, G., Adamski, M., Aitken, N., Banks, S., Ingwersen, D., Ranjard, L., Rayner, L., Stojanovic, D., Suchan, T., von Takach Dukai, B., & Heinsohn, R. (2019). Genomic impact of severe population decline in a nomadic songbird. *PLOS ONE*, *14*(10), e0223953. https://doi.org/10.1371/journal.pone.0223953

Cruz-Dávalos, D. I., Llamas, B., Gaunitz, C., Fages, A., Gamba, C., Soubrier, J., Librado, P., Seguin-Orlando, A., Pruvost, M., Alfarhan, A. H., Alquraishi, S. A., Al-Rasheid, K. A. S., Scheu, A., Beneke, N., Ludwig, A., Cooper, A., Willerslev, E., & Orlando, L. (2017). Experimental conditions improving in-solution target enrichment for ancient DNA. *Molecular Ecology Resources*, *17*(3), 508–522. https://doi.org/10.1111/1755-0998.12595

Dabney, J., Meyer, M., & Pääbo, S. (2013). Ancient DNA damage. *Cold Spring Harbor Perspectives in Biology*, *5*(7). https://doi.org/10.1101/cshperspect.a012567

Daley, T., & Smith, A. D. (2013). Predicting the molecular complexity of sequencing libraries. *Nature Methods*, *10*(4), 325–327. https://doi.org/10.1038/nmeth.2375

Danecek, P., Auton, A., Abecasis, G., Albers, C. A., Banks, E., DePristo, M. A., Handsaker, R. E., Lunter, G., Marth, G. T., Sherry, S. T., McVean, G., Durbin, R., & 1000 Genomes Project Analysis Group. (2011). The variant call format and VCFtools. *Bioinformatics*, *27*(15), 2156–2158. https://doi.org/10.1093/bioinformatics/btr330

Enk, J. M., Devault, A. M., Kuch, M., Murgha, Y. E., Rouillard, J.-M., & Poinar, H. N. (2014). Ancient Whole Genome Enrichment Using Baits Built from Modern DNA. *Molecular Biology and Evolution*, *31*(5), 1292–1294. https://doi.org/10.1093/molbev/msu074

Fages, A., Hanghøj, K., Khan, N., Gaunitz, C., Seguin-Orlando, A., Leonardi, M., McCrory Constantz, C., Gamba, C., Al-Rasheid, K. A. S., Albizuri, S., Alfarhan, A. H., Allentoft, M., Alquraishi, S., Anthony, D., Baimukhanov, N., Barrett, J. H., Bayarsaikhan, J., Benecke, N.,

Bernáldez-Sánchez, E., … Orlando, L. (2019). Tracking Five Millennia of Horse Management with Extensive Ancient Genome Time Series. *Cell*, *177*(6), 1419-1435.e31. https://doi.org/10.1016/j.cell.2019.03.049

Fontsere, C., Alvarez-Estape, M., Lester, J., Arandjelovic, M., Kuhlwilm, M., Dieguez, P., Agbor, A., Angedakin, S., Ayuk Ayimisin, E., Bessone, M., Brazzola, G., Deschner, T., Eno-Nku, M., Granjon, A., Head, J., Kadam, P., Kalan, A. K., Kambi, M., Langergraber, K., … Lizano, E. (2020). Maximizing the acquisition of unique reads in noninvasive capture sequencing experiments. *Molecular Ecology Resources*, 1755-0998.13300. https://doi.org/10.1111/1755-0998.13300

Furtwängler, A., Neukamm, J., Böhme, L., Reiter, E., Vollstedt, M., Arora, N., Singh, P., Cole, S. T., Knauf, S., Calvignac-Spencer, S., Krause-Kyora, B., Krause, J., Schuenemann, V. J., & Herbig, A. (2020). Comparison of target enrichment strategies for ancient pathogen DNA. *BioTechniques*, *69*(6), 455–459. https://doi.org/10.2144/btn-2020-0100

Gamba, C., Hanghøj, K., Gaunitz, C., Alfarhan, A. H., Alquraishi, S. A., Al-Rasheid, K. A. S., Bradley, D. G., & Orlando, L. (2016). Comparing the performance of three ancient DNA extraction methods for high-throughput sequencing. *Molecular Ecology Resources*, *16*(2), 459–469. https://doi.org/10.1111/1755-0998.12470

Garrison, E., & Marth, G. (2012). Haplotype-based variant detection from short-read sequencing. *ArXiv:1207.3907 [q-Bio]*. http://arxiv.org/abs/1207.3907

Gauthier, J., Pajkovic, M., Neuenschwander, S., Kaila, L., Schmid, S., Orlando, L., & Alvarez, N. (2020). Museomics identifies genetic erosion in two butterfly species across the 20th century in Finland. *Molecular Ecology Resources*, *20*(5), 1191–1205. https://doi.org/10.1111/1755-0998.13167

Giguet-Covex, C., Pansu, J., Arnaud, F., Rey, P.-J., Griggo, C., Gielly, L., Domaizon, I., Coissac, E., David, F., Choler, P., Poulenard, J., & Taberlet, P. (2014). Long livestock farming history and human landscape shaping revealed by lake sediment DNA. *Nature Communications*, *5*(1), 3211. https://doi.org/10.1038/ncomms4211

Goodwin, S., McPherson, J. D., & McCombie, W. R. (2016). Coming of age: Ten years of next-generation sequencing technologies. *Nature Reviews Genetics*, *17*(6), 333–351. https://doi.org/10.1038/nrg.2016.49

Hanghøj, K., Seguin-Orlando, A., Schubert, M., Madsen, T., Pedersen, J. S., Willerslev, E., & Orlando, L. (2016). Fast, Accurate and Automatic Ancient Nucleosome and Methylation Maps with epiPALEOMIX. *Molecular Biology and Evolution*, *33*(12), 3284–3298. https://doi.org/10.1093/molbev/msw184

Hernandez-Rodriguez, J., Arandjelovic, M., Lester, J., de Filippo, C., Weihmann, A., Meyer, M., Angedakin, S., Casals, F., Navarro, A., Vigilant, L., Kühl, H. S., Langergraber, K., Boesch, C., Hughes, D., & Marques-Bonet, T. (2018). The impact of endogenous content, replicates and pooling on genome capture from faecal samples. *Molecular Ecology Resources*, *18*(2), 319–333. https://doi.org/10.1111/1755-0998.12728

Holland, I., & Davies, J. A. (2020). Automation in the Life Science Research Laboratory. *Frontiers in Bioengineering and Biotechnology*, *8*, 571777. https://doi.org/10.3389/fbioe.2020.571777

Jónsson, H., Ginolhac, A., Schubert, M., Johnson, P. L. F., & Orlando, L. (2013). mapDamage2.0: Fast approximate Bayesian estimates of ancient DNA damage parameters. *Bioinformatics*, *29*(13), 1682–1684. https://doi.org/10.1093/bioinformatics/btt193

635 Kalbfleisch, T. S., Rice, E. S., DePriest, M. S., Walenz, B. P., Hestand, M. S., Vermeesch, J.
636 R., O Connell, B. L., Fiddes, I. T., Vershinina, A. O., Saremi, N. F., Petersen, J. L., Finno, C.
637 J., Bellone, R. R., McCue, M. E., Brooks, S. A., Bailey, E., Orlando, L., Green, R. E., Miller,
638 D. C., … MacLeod, J. N. (2018). Improved reference genome for the domestic horse
639 increases assembly contiguity and composition. *Communications Biology*, *1*, 197.
640 https://doi.org/10.1038/s42003-018-0199-z

641 Karam, M.-J., Lefèvre, F., Dagher-Kharrat, M. B., Pinosio, S., & Vendramin, G. G. (2015).
642 Genomic exploration and molecular marker development in a large and complex conifer
643 genome using RADseq and mRNAseq. *Molecular Ecology Resources*, *15*(3), 601–612.
644 https://doi.org/10.1111/1755-0998.12329

645 Kozarewa, I., Armisen, J., Gardner, A. F., Slatko, B. E., & Hendrickson, C. L. (2015).
646 Overview of Target Enrichment Strategies. *Current Protocols in Molecular Biology*, *112*(1).
647 https://doi.org/10.1002/0471142727.mb0721s112

648 Lang, P. L. M., Weiß, C. L., Kersten, S., Latorre, S. M., Nagel, S., Nickel, B., Meyer, M., &
649 Burbano, H. A. (2020). Hybridization ddRAD-sequencing for population genomics of
650 nonmodel plants using highly degraded historical specimen DNA. *Molecular Ecology*
651 *Resources*, *20*(5), 1228–1247. https://doi.org/10.1111/1755-0998.13168

652 Langmead, B., & Salzberg, S. L. (2012). Fast gapped-read alignment with Bowtie 2. *Nature*
653 *Methods*, *9*(4), 357–359. https://doi.org/10.1038/nmeth.1923

654 Larsson, H., De Paoli, E., Morgante, M., Lascoux, M., & Gyllenstrand, N. (2013). The
655 Hypomethylated Partial Restriction (HMPR) method reduces the repetitive content of
656 genomic libraries in Norway spruce (Picea abies). *Tree Genetics & Genomes*, *9*(2), 601–612.
657 https://doi.org/10.1007/s11295-012-0582-8

658 Leonardi, M., Librado, P., Der Sarkissian, C., Schubert, M., Alfarhan, A. H., Alquraishi, S.
659 A., Al-Rasheid, K. A. S., Gamba, C., Willerslev, E., & Orlando, L. (2016). Evolutionary
660 Patterns and Processes: Lessons from Ancient DNA. *Systematic Biology*, syw059.
661 https://doi.org/10.1093/sysbio/syw059

662 Lesnik, E. A., & Freier, S. M. (1995). Relative Thermodynamic Stability of DNA, RNA, and
663 DNA:RNA Hybrid Duplexes: Relationship with Base Composition and Structure.
664 *Biochemistry*, *34*(34), 10807–10815. https://doi.org/10.1021/bi00034a013

665 Li, H., Handsaker, B., Wysoker, A., Fennell, T., Ruan, J., Homer, N., Marth, G., Abecasis, G.,
666 Durbin, R., & 1000 Genome Project Data Processing Subgroup. (2009). The Sequence
667 Alignment/Map format and SAMtools. *Bioinformatics*, *25*(16), 2078–2079.
668 https://doi.org/10.1093/bioinformatics/btp352

669 Linck, E. B., Hanna, Z. R., Sellas, A., & Dumbacher, J. P. (2017). Evaluating hybridization
670 capture with RAD probes as a tool for museum genomics with historical bird specimens.
671 *Ecology and Evolution*, *7*(13), 4755–4767. https://doi.org/10.1002/ece3.3065

672 Mamanova, L., Coffey, A. J., Scott, C. E., Kozarewa, I., Turner, E. H., Kumar, A., Howard,
673 E., Shendure, J., & Turner, D. J. (2010). Target-enrichment strategies for next-generation
674 sequencing. *Nature Methods*, *7*(2), 111–118. https://doi.org/10.1038/nmeth.1419

675 Maricic, T., Whitten, M., & Pääbo, S. (2010). Multiplexed DNA Sequence Capture of
676 Mitochondrial Genomes Using PCR Products. *PLoS ONE*, *5*(11), e14004.
677 https://doi.org/10.1371/journal.pone.0014004

678 Martin, M. (2011). Cutadapt removes adapter sequences from high-throughput sequencing
679 reads. *EMBnet.Journal*, *17*(1), 10. https://doi.org/10.14806/ej.17.1.200

Mathieson, I., Lazaridis, I., Rohland, N., Mallick, S., Patterson, N., Roodenberg, S. A., Harney, E., Stewardson, K., Fernandes, D., Novak, M., Sirak, K., Gamba, C., Jones, E. R., Llamas, B., Dryomov, S., Pickrell, J., Arsuaga, J. L., de Castro, J. M. B., Carbonell, E., … Reich, D. (2015). Genome-wide patterns of selection in 230 ancient Eurasians. *Nature*, *528*(7583), 499–503. https://doi.org/10.1038/nature16152

May, M. (2019). A DIY approach to automating your lab. *Nature*, *569*(7757), 587–588. https://doi.org/10.1038/d41586-019-01590-z

McCormack, J. E., Hird, S. M., Zellmer, A. J., Carstens, B. C., & Brumfield, R. T. (2013). Applications of next-generation sequencing to phylogeography and phylogenetics. *Molecular Phylogenetics and Evolution*, *66*(2), 526–538. https://doi.org/10.1016/j.ympev.2011.12.007

Meyer, M., & Kircher, M. (2010). Illumina Sequencing Library Preparation for Highly Multiplexed Target Capture and Sequencing. *Cold Spring Harbor Protocols*, *2010*(6), pdb.prot5448. https://doi.org/10.1101/pdb.prot5448

Orlando, L. (2020). The Evolutionary and Historical Foundation of the Modern Horse: Lessons from Ancient Genomics. *Annual Review of Genetics*, *54*, 563–581. https://doi.org/10.1146/annurev-genet-021920-011805

Orlando, L., & Cooper, A. (2014). Using Ancient DNA to Understand Evolutionary and Ecological Processes. *Annual Review of Ecology, Evolution, and Systematics*, *45*(1), 573–598. https://doi.org/10.1146/annurev-ecolsys-120213-091712

Orlando, L., Ginolhac, A., Zhang, G., Froese, D., Albrechtsen, A., Stiller, M., Schubert, M., Cappellini, E., Petersen, B., Moltke, I., Johnson, P. L. F., Fumagalli, M., Vilstrup, J. T., Raghavan, M., Korneliussen, T., Malaspinas, A.-S., Vogt, J., Szklarczyk, D., Kelstrup, C. D., … Willerslev, E. (2013). Recalibrating Equus evolution using the genome sequence of an early Middle Pleistocene horse. *Nature*, *499*(7456), 74–78. https://doi.org/10.1038/nature12323

Pedersen, M. W., Ruter, A., Schweger, C., Friebe, H., Staff, R. A., Kjeldsen, K. K., Mendoza, M. L. Z., Beaudoin, A. B., Zutter, C., Larsen, N. K., Potter, B. A., Nielsen, R., Rainville, R. A., Orlando, L., Meltzer, D. J., Kjær, K. H., & Willerslev, E. (2016). Postglacial viability and colonization in North America's ice-free corridor. *Nature*, *537*(7618), 45–49. https://doi.org/10.1038/nature19085

Peñalba, J. V., Smith, L. L., Tonione, M. A., Sass, C., Hykin, S. M., Skipwith, P. L., McGuire, J. A., Bowie, R. C. K., & Moritz, C. (2014). Sequence capture using PCR-generated probes: A cost-effective method of targeted high-throughput sequencing for nonmodel organisms. *Molecular Ecology Resources*, n/a-n/a. https://doi.org/10.1111/1755-0998.12249

Peterson, B. K., Weber, J. N., Kay, E. H., Fisher, H. S., & Hoekstra, H. E. (2012). Double Digest RADseq: An Inexpensive Method for De Novo SNP Discovery and Genotyping in Model and Non-Model Species. *PLoS ONE*, *7*(5), e37135. https://doi.org/10.1371/journal.pone.0037135

Poullet, M., & Orlando, L. (2020). Assessing DNA Sequence Alignment Methods for Characterizing Ancient Genomes and Methylomes. *Frontiers in Ecology and Evolution*, *8*, 105. https://doi.org/10.3389/fevo.2020.00105

Prüfer, K., Stenzel, U., Hofreiter, M., Pääbo, S., Kelso, J., & Green, R. E. (2010). Computational challenges in the analysis of ancient DNA. *Genome Biology*, *11*(5), R47. https://doi.org/10.1186/gb-2010-11-5-r47

725 Quinlan, A. R., & Hall, I. M. (2010). BEDTools: A flexible suite of utilities for comparing
726 genomic features. *Bioinformatics*, *26*(6), 841–842.
727 https://doi.org/10.1093/bioinformatics/btq033

728 Rohland, N., Harney, E., Mallick, S., Nordenfelt, S., & Reich, D. (2015). Partial uracil–
729 DNA–glycosylase treatment for screening of ancient DNA. *Philosophical Transactions of the*
730 *Royal Society B: Biological Sciences*, *370*(1660), 20130624.
731 https://doi.org/10.1098/rstb.2013.0624

732 Schmid, S., Genevest, R., Gobet, E., Suchan, T., Sperisen, C., Tinner, W., & Alvarez, N.
733 (2017). HyRAD-X, a versatile method combining exome capture and RAD sequencing to
734 extract genomic information from ancient DNA. *Methods in Ecology and Evolution*, *8*(10),
735 1374–1388. https://doi.org/10.1111/2041-210X.12785

736 Schmid, S., Neuenschwander, S., Pitteloud, C., Heckel, G., Pajkovic, M., Arlettaz, R., &
737 Alvarez, N. (2018). Spatial and temporal genetic dynamics of the grasshopper Oedaleus
738 decorus revealed by museum genomics. *Ecology and Evolution*, *8*(3), 1480–1495.
739 https://doi.org/10.1002/ece3.3699

740 Schubert, M., Ermini, L., Sarkissian, C. D., Jónsson, H., Ginolhac, A., Schaefer, R., Martin,
741 M. D., Fernández, R., Kircher, M., McCue, M., Willerslev, E., & Orlando, L. (2014).
742 Characterization of ancient and modern genomes by SNP detection and phylogenomic and
743 metagenomic analysis using PALEOMIX. *Nature Protocols*, *9*(5), 1056–1082.
744 https://doi.org/10.1038/nprot.2014.063

745 Schubert, M., Lindgreen, S., & Orlando, L. (2016). AdapterRemoval v2: Rapid adapter
746 trimming, identification, and read merging. *BMC Research Notes*, *9*(1), 88.
747 https://doi.org/10.1186/s13104-016-1900-2

748 Seguin-Orlando, A., Gamba, C., Sarkissian, C. D., Ermini, L., Louvel, G., Boulygina, E.,
749 Sokolov, A., Nedoluzhko, A., Lorenzen, E. D., Lopez, P., McDonald, H. G., Scott, E.,
750 Tikhonov, A., Stafford, T. W., Alfarhan, A. H., Alquraishi, S. A., Al-Rasheid, K. A. S.,
751 Shapiro, B., Willerslev, E., … Orlando, L. (2015). Pros and cons of methylation-based
752 enrichment methods for ancient DNA. *Scientific Reports*, *5*(1), 11826.
753 https://doi.org/10.1038/srep11826

754 Skoglund, P., Northoff, B. H., Shunkov, M. V., Derevianko, A. P., Pääbo, S., Krause, J., &
755 Jakobsson, M. (2014). Separating endogenous ancient DNA from modern day contamination
756 in a Siberian Neandertal. *Proceedings of the National Academy of Sciences*, *111*(6), 2229–
757 2234. https://doi.org/10.1073/pnas.1318934111

758 Slon, V., Hopfe, C., Weiß, C. L., Mafessoni, F., de la Rasilla, M., Lalueza-Fox, C., Rosas, A.,
759 Soressi, M., Knul, M. V., Miller, R., Stewart, J. R., Derevianko, A. P., Jacobs, Z., Li, B.,
760 Roberts, R. G., Shunkov, M. V., de Lumley, H., Perrenoud, C., Gušić, I., … Meyer, M.
761 (2017). Neandertal and Denisovan DNA from Pleistocene sediments. *Science*, *356*(6338),
762 605–608. https://doi.org/10.1126/science.aam9695

763 Smith, O., Clapham, A. J., Rose, P., Liu, Y., Wang, J., & Allaby, R. G. (2015). Genomic
764 methylation patterns in archaeological barley show de-methylation as a time-dependent
765 diagenetic process. *Scientific Reports*, *4*(1), 5559. https://doi.org/10.1038/srep05559

766 Suchan, T., Pitteloud, C., Gerasimova, N. S., Kostikova, A., Schmid, S., Arrigo, N., Pajkovic,
767 M., Ronikier, M., & Alvarez, N. (2016). Hybridization Capture Using RAD Probes (hyRAD),
768 a New Tool for Performing Genomic Analyses on Collection Specimens. *PLOS ONE*, *11*(3),
769 e0151651. https://doi.org/10.1371/journal.pone.0151651

van der Valk, T., Pečnerová, P., Díez-del-Molino, D., Bergström, A., Oppenheimer, J., Hartmann, S., Xenikoudakis, G., Thomas, J. A., Dehasque, M., Sağlıcan, E., Fidan, F. R., Barnes, I., Liu, S., Somel, M., Heintzman, P. D., Nikolskiy, P., Shapiro, B., Skoglund, P., Hofreiter, M., … Dalén, L. (2021). Million-year-old DNA sheds light on the genomic history of mammoths. *Nature*, *591*(7849), 265–269. https://doi.org/10.1038/s41586-021-03224-9

Wilcox, T. M., Zarn, K. E., Piggott, M. P., Young, M. K., McKelvey, K. S., & Schwartz, M. K. (2018). Capture enrichment of aquatic environmental DNA: A first proof of concept. *Molecular Ecology Resources*, *18*(6), 1392–1401. https://doi.org/10.1111/1755-0998.12928

Willerslev, E., Davison, J., Moora, M., Zobel, M., Coissac, E., Edwards, M. E., Lorenzen, E. D., Vestergård, M., Gussarova, G., Haile, J., Craine, J., Gielly, L., Boessenkool, S., Epp, L. S., Pearman, P. B., Cheddadi, R., Murray, D., Bråthen, K. A., Yoccoz, N., … Taberlet, P. (2014). Fifty thousand years of Arctic vegetation and megafaunal diet. *Nature*, *506*(7486), 47–51. https://doi.org/10.1038/nature12921

Tables and figures

Tab. 1 Samples used in the study and endogenous DNA content prior to capture. BCE = Before Common Era. CE = Common Era. BP = Before Present. Uncal = uncalibrated radiocarbon range.

Sample name	Sample age	Site	Material	Endogenous DNA content (all/unique)
PLMie10	Lusatian culture, Bronze Age/Early Iron Age (1,200-600 BCE)	Miechów, Poland	metatarsus	0.34/0.34%
PLSla2	Funnelbeaker culture, Eneolithic (3,700-3,000 BCE)	Sławęcinek, Poland	molar	0.51/0.51%
PLMie8	Found in Funnelbeaker culture feature, Eneolithic (3,700-3,000 BCE)	Miechów, Poland	metacarpus	6.58/6.55%
DIV9	Upper Paleolithic, Late Glacial period (13,000-14,500 uncal BP)	Divnogor'ye, Voronezh Region, Russia	molar	27.42/1.72%
KB217	Upper Paleolithic	Medvezhiya cave, upper course of the river Pechora, Urals, Russia	metapodium	16.83/11.20%
PLMie3	Przeworsk culture, Roman period (1^{st}-4^{th} century CE)	Miechów, Poland	femur	13.09/13.85%
LOG3	Upper Paleolithic (infinite ^{14}C date, >52,200 uncal BP)	Hyena's Lair, Altai Republic, Russia	metatarsus	20.64/20.55%
SV2019-22	Iron Age, Middle Numidian period (5^{th}-6^{th} century BCE)	Althiburos, Tunisia	tooth	33.84/33.66%
SV2019-18	Iron Age, Middle Numidian period (5^{th}-6^{th} century BCE)	Althiburos, Tunisia	tooth	47.19/46.97%
PLKaz4	Trzciniec culture, Early Bronze Age (1,900-1,200 BCE)	Kazimierza Wielka, Poland	petrous temporal bone	51.67/51.48%
PLKaz1	Trzciniec culture, Early Bronze Age (1900-1,200 BCE)	Kazimierza Wielka, Poland	petrous temporal bone	60.43/60.15%
PLKaz2	Trzciniec culture, Early Bronze Age (1,900-1,200 BCE)	Kazimierza Wielka, Poland	petrous temporal bone	73.78/73.59%

789 Tab. 2 Sequence characteristics for the sequenced probes libraries (**in-silico* estimation for
790 *HpaII-MseI* probes does not take methylation-sensitivity into account).

Enzyme combination	Raw reads	Properly paired reads	Number of multimapping properly paired reads	Number of targets	Number of targets after merging overlapping targets	Percent of the genome targeted	Percent of the genome predicted *in silico*
PstI-MseI	502,815	380,495	43,713	247,716	246,973	1.81%	4.77%
MspI-MseI	502,815	381,803	55,672	260,579	257,588	2.07%	7.16%
HpaII-MseI	502,815	387,275	32,569	234,924	223,789	1.55%	7.16%*

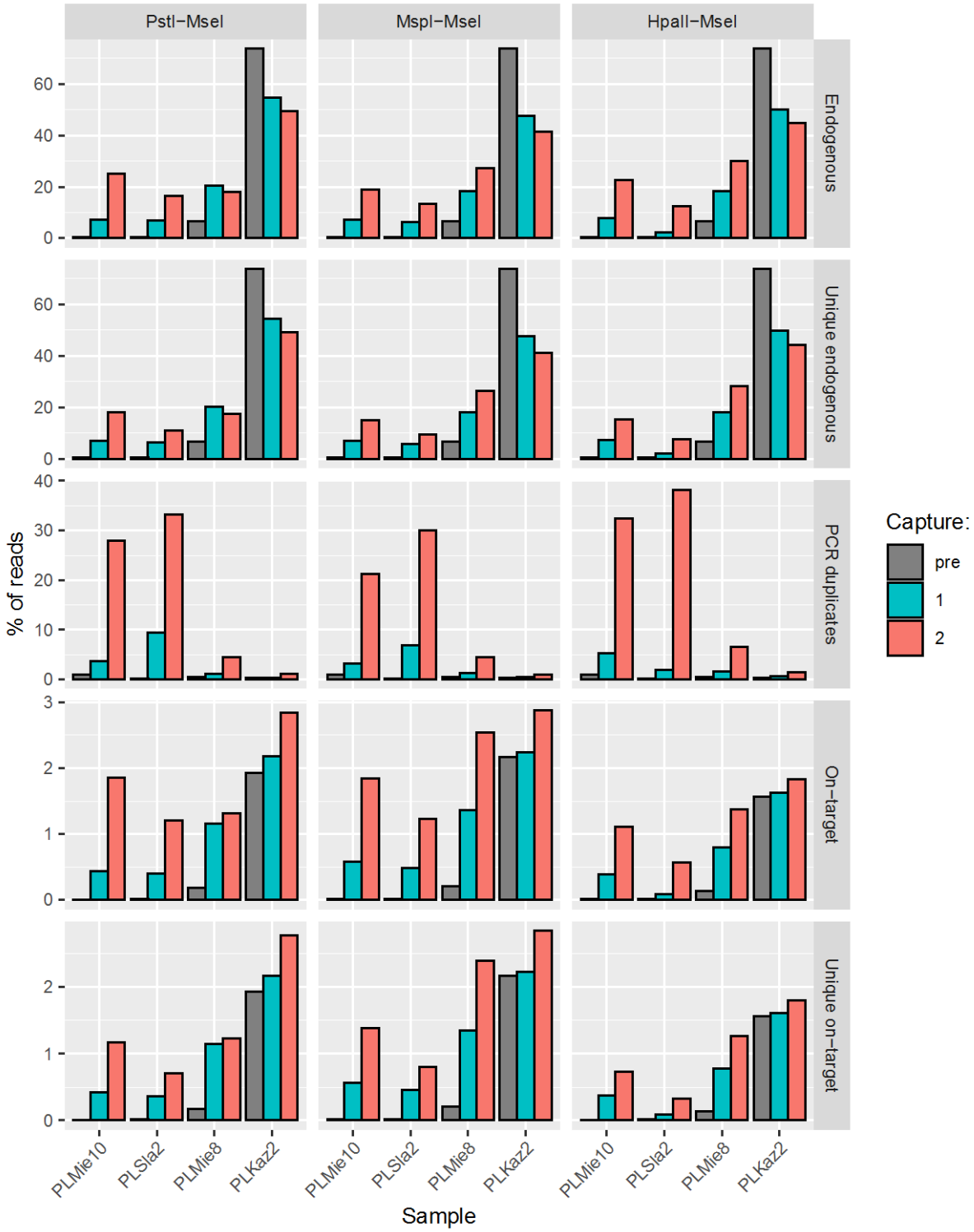

Fig. 1 Percentage of endogenous, unique endogenous (after removing PCR duplicates), reads flagged as PCR duplicates, on-target reads (i.e. overlapping by at least 1 nt with the target regions), and unique on-target reads. Results are shown for shotgun genomic libraries (pre) and the same libraries with one (capture 1) or two rounds (capture 2) of capture with three types of hyRAD probes, filtering for a minimum mapping quality of 25 (analyses relaxing the mapping quality filter are shown in Fig. S10 so as to illustrate the impact of repeated elements in the sequence data).

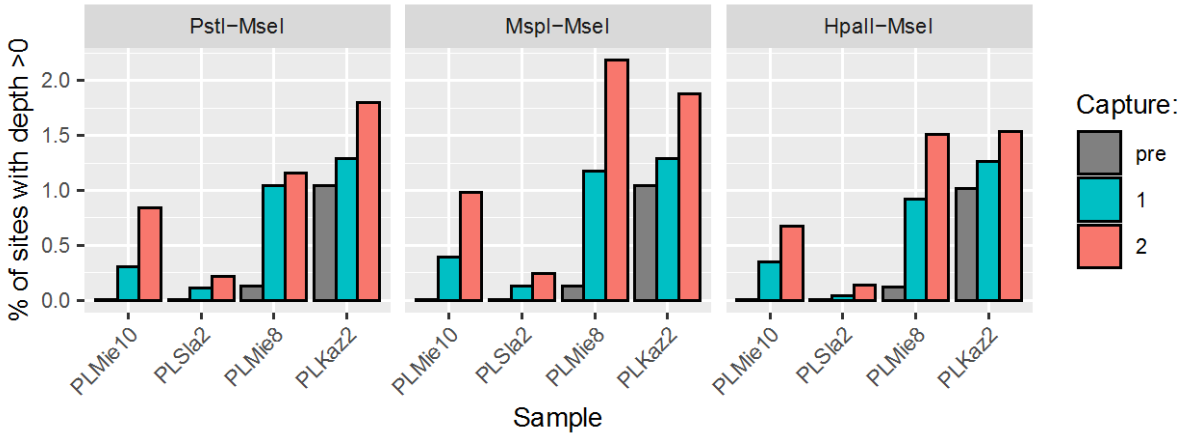

Fig. 2 Percentage of sites with non-null coverage, considering unique on-target reads. Results are shown for shotgun genomic libraries (pre) and the same libraries with one (capture 1) or two rounds (capture 2) of capture with the three types of hyRAD probes.

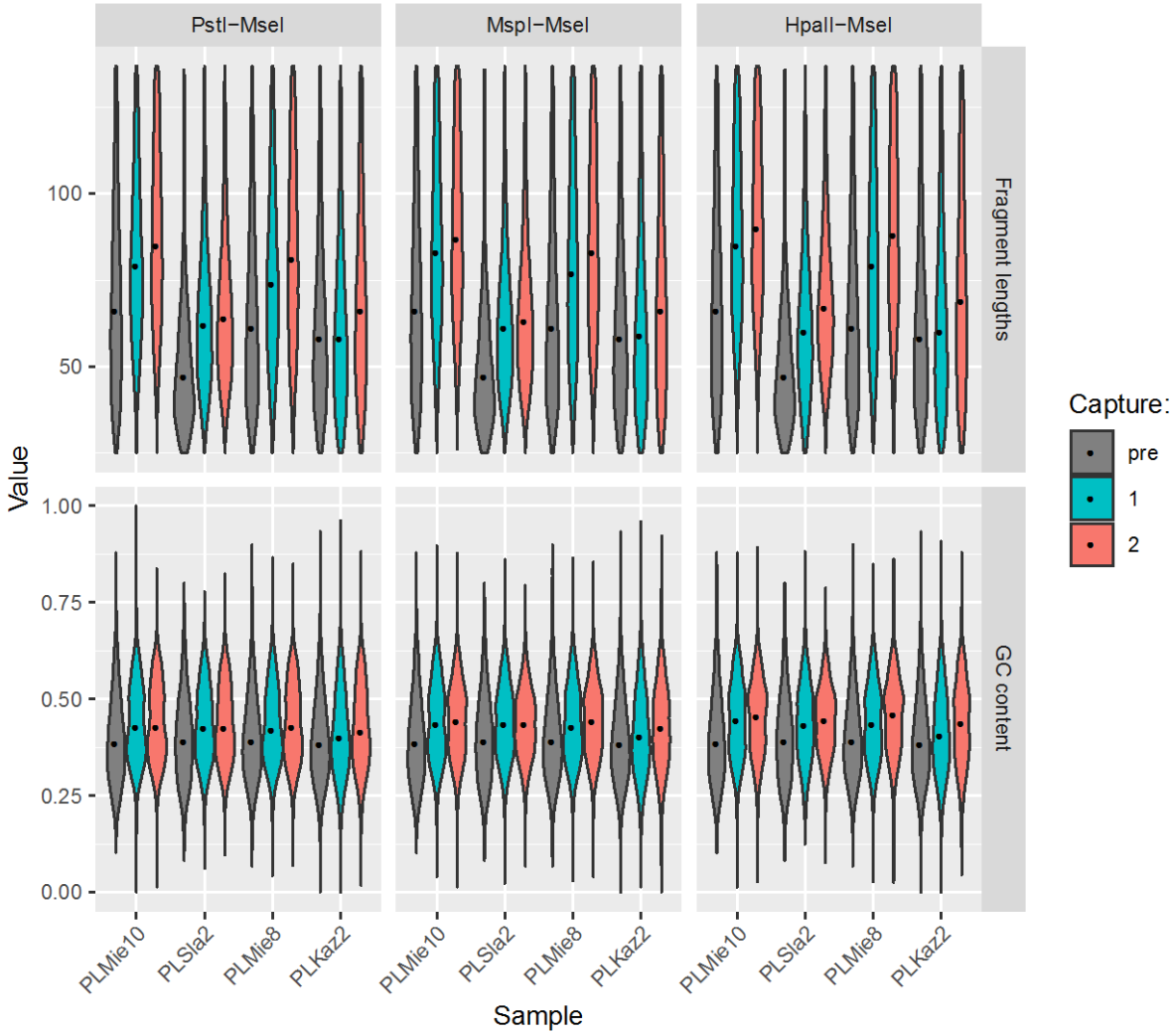

Fig. 3 The effect of one (capture 1) or two rounds (capture 2) of capture with three types of hyRAD probes on the %GC content and sequenced fragment lengths, as compared with the shotgun libraries (pre).

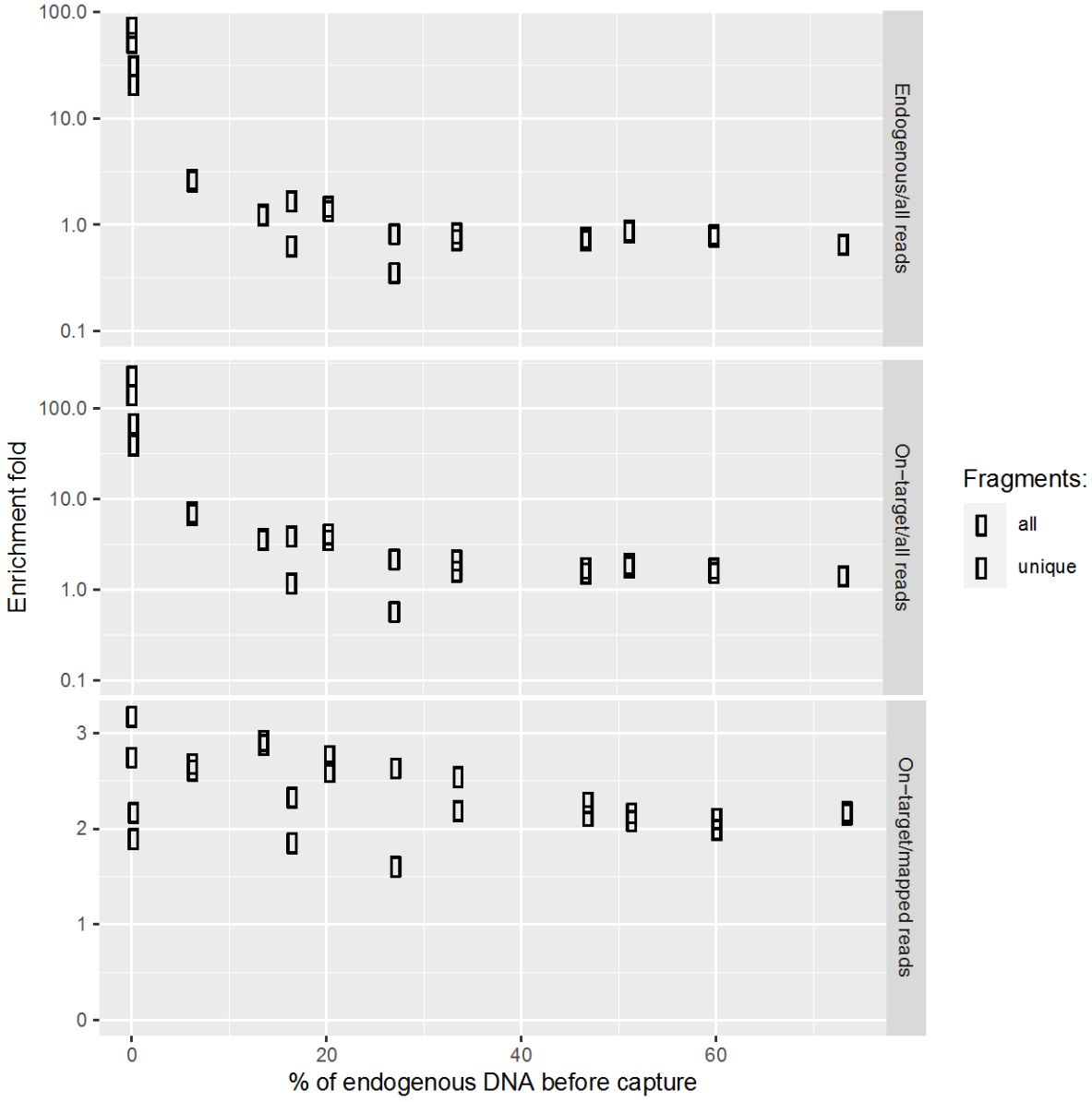

808

809

810 Fig.4 Enrichment-folds for 12 samples enriched in two consecutive rounds on *PstI-MseI*
811 probes, for all and unique fragments (*i.e.* after PCR duplicate removal). The enrichment is
812 calculated as the proportion of mapped-to-all reads, on-target-to-all reads, and on-target-to-
813 mapped reads. Note that two top panels are in *log*-scale.

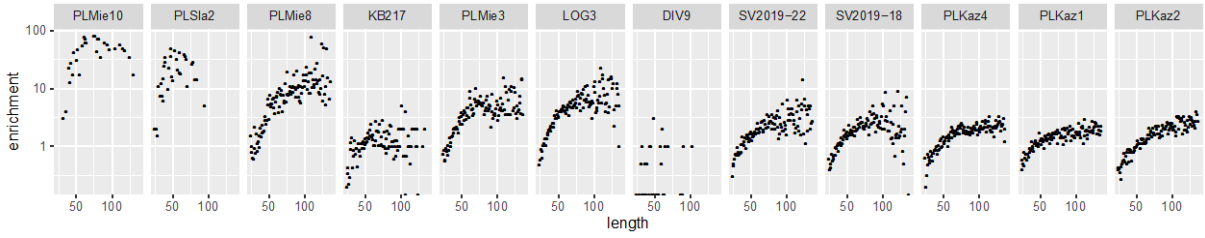

814

815 Fig. 5 Enrichment-folds as a function of the fragment length for 12 samples enriched in two
816 consecutive rounds on *PstI-MseI* probes.

817

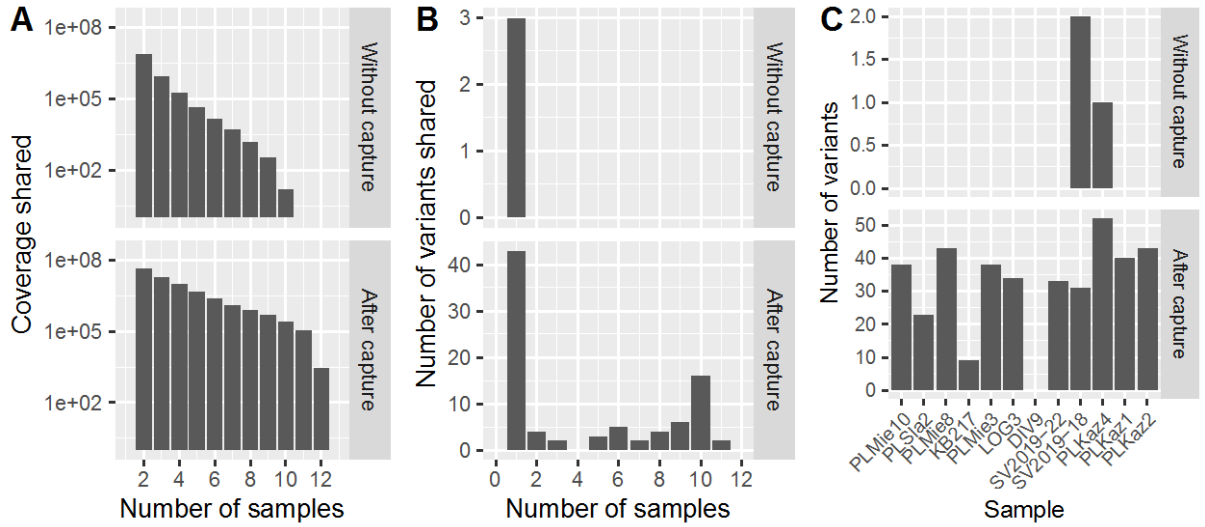

818

819 Fig. 6 A) Number of mapped nucleotides shared by *n* samples without and after two
820 consecutive rounds on *PstI-MseI* probes. Note the *log* scale on the *y* axis; B) Number of
821 shared genomic variants shared by *n* samples without and after two consecutive rounds on
822 *PstI-MseI* probes; C) Number of genomic variants detected in each sample without and after
823 two consecutive rounds on *PstI-MseI* probes. Note that the scales of upper and lower panel
824 are different for both panels B and C.

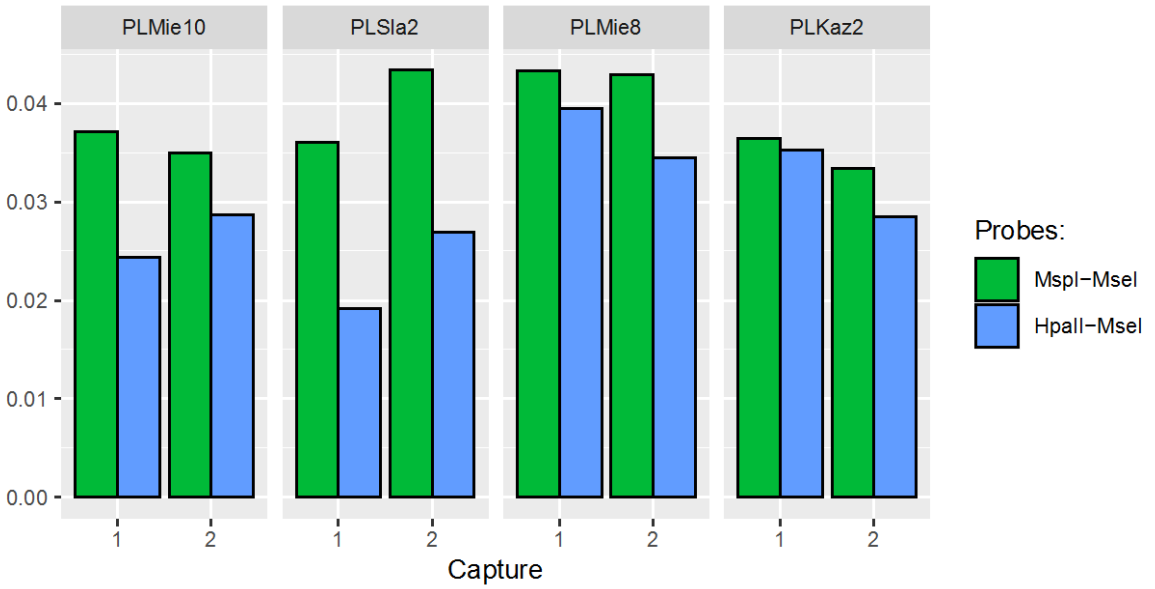

825

826 Fig. 7 Postmortem DNA damage estimates of the unique on-target reads after one and two
827 rounds of capture on *MspI-MseI vs HpaII-MseI* probes. The plot shows 5'-end cytosine
828 deamination rates in CpG context as estimated by PMDtools and cumulated across the first 10
829 read positions.

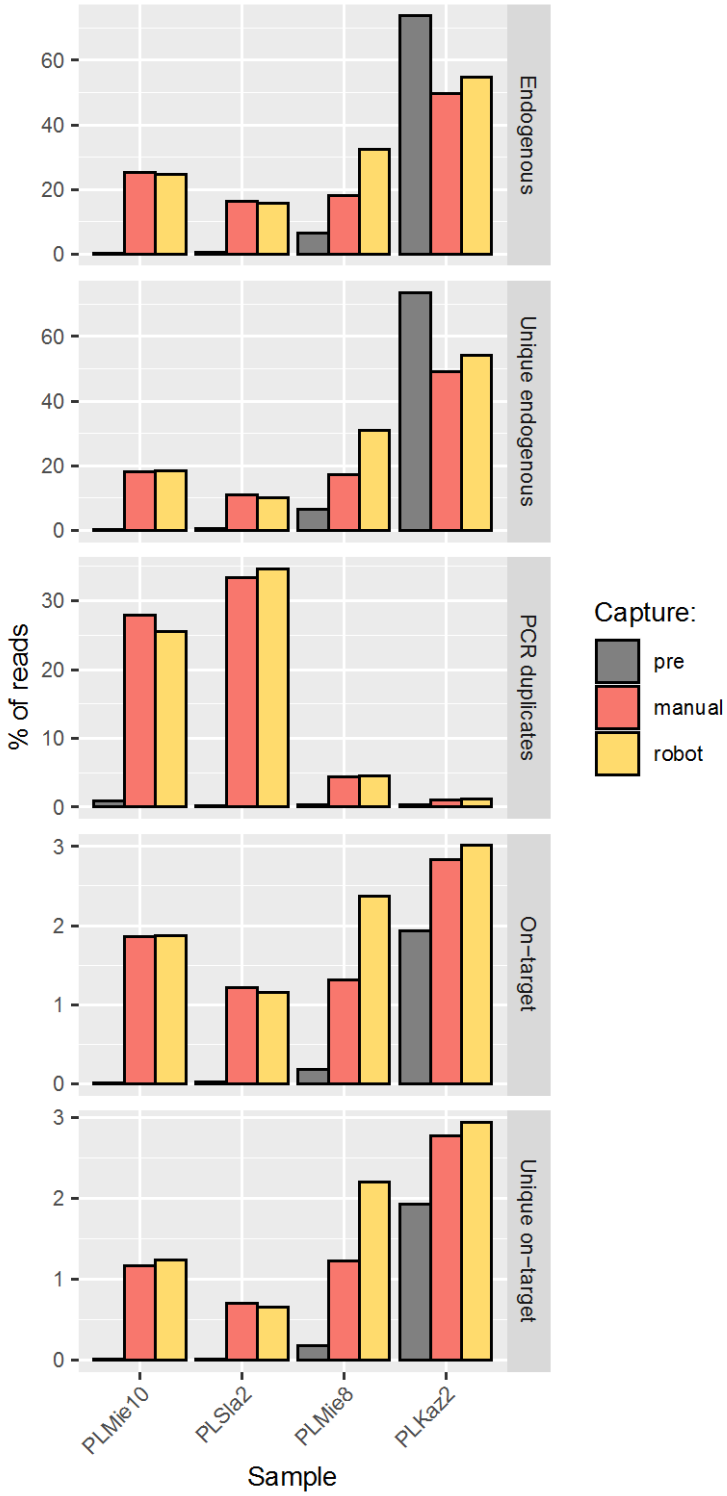

830

831 Fig. 8 Percentage of endogenous, unique endogenous reads, reads flagged as PCR duplicates,
832 on-target reads, and unique on-target reads as compared between manual and robotic capture
833 procedure, using *PstI-MseI* probes.